Assessment of Segmental Myocardial Blood Flow and Myocardial Perfusion Reserve by Adenosine-Stress Myocardial Arterial Spin Labeling Perfusion Imaging

Andrew J. Yoon, MD,[1]* Hung Phi Do, PhD,[2] Steven Cen, PhD,[3] Michael W. Fong, MD,[1] Farhood Saremi, MD,[3] Mark L. Barr, MD,[4] and Krishna S. Nayak, PhD[5]

Purpose: To determine the feasibility of measuring increases in myocardial blood flow (MBF) and myocardial perfusion reserve (MPR) on a per-segment basis using arterial spin labeled (ASL) magnetic resonance imaging (MRI) with adenosine vasodilator stress in normal human myocardium.
Materials and Methods: Myocardial ASL scans at rest and during adenosine infusion were incorporated into a routine 3T MR adenosine-induced vasodilator stress protocol and were performed in 10 healthy human volunteers. Myocardial ASL was performed using single-gated flow-sensitive alternating inversion recovery (FAIR) tagging and balanced steady-state free precession (bSSFP) imaging at 3T. A T_2-prep blood oxygen level-dependent (BOLD) SSFP sequence was used to concurrently assess segmental myocardial oxygenation with BOLD signal intensity (SI) percent change in the same subjects.
Results: There was a statistically significant difference between MBF measured by ASL at rest (1.75 ± 0.86 ml/g/min) compared to adenosine stress (4.58 ± 2.14 ml/g/min) for all wall segments ($P < 0.0001$), yielding a per-segment MPR of 3.02 ± 1.51. When wall segments were divided into specific segmental myocardial perfusion territories (ie, anteroseptal, anterior, anterolateral, inferolateral, inferior, and inferoseptal), the differences between rest and stress regional MBF for each territory remained consistently statistically significant ($P < 0.001$) after correcting for multiple comparisons.
Conclusion: This study demonstrates the feasibility of measuring MBF and MPR on a segmental basis by single-gated cardiac ASL in normal volunteers. Second, this study demonstrates the feasibility of performing the ASL sequence and T_2-prepared SSFP BOLD imaging during a single adenosine infusion.
Level of Evidence: 2
Technical Efficacy: Stage 1

J. MAGN. RESON. IMAGING 2017;46:413–420

MYOCARDIAL PERFUSION and myocardial perfusion reserve are important measures used for the diagnosis and risk-stratification of patients with coronary artery disease (CAD).[1,2] First-pass perfusion magnetic resonance imaging (MRI) has improved sensitivity and specificity compared to SPECT perfusion imaging,[3] but requires the use of gadolinium-based contrast agents that are potentially toxic to patients with renal dysfunction.[4] Arterial spin labeling (ASL) is a quantitative, noncontrast MRI technique that uses blood itself as the signal tracer to measure tissue perfusion, and can be safely applied to patients repeatedly.[5]

ASL is most commonly used in the brain for the clinical quantification of cerebral blood flow in cerebrovascular disease and neuro-oncology,[5–7] but much work has been done over the past decade to adapt and develop ASL for use in the quantification of blood flow in other organs,

View this article online at wileyonlinelibrary.com. DOI: 10.1002/jmri.25604

Received Sep 21, 2016, Accepted for publication Dec 5, 2016.

*Address reprint requests to: A.J.Y., Department of Medicine, Division of Cardiology, Keck School of Medicine of USC, 1510 San Pablo St., Ste. 322, Los Angeles, CA 90033. E-mail: Andrew.yoon@med.usc.edu

From the [1]Department of Medicine, Division of Cardiology, Keck School of Medicine of USC, University of Southern California, Los Angeles, California, USA; [2]Department of Physics and Astronomy, University of Southern California, Los Angeles, California, USA; [3]Department of Radiology, Keck School of Medicine of USC, University of Southern California, Los Angeles, California, USA; [4]Department of Cardiothoracic Surgery, Keck School of Medicine of USC, University of Southern California, Los Angeles, California, USA; and [5]Ming Hsieh Department of Electrical Engineering, University of Southern California, Los Angeles, California, USA

including myocardial blood flow (MBF) in both animal[8–16] and human models.[17–20] Myocardial ASL is compatible with pharmacological stress testing and is able to detect clinically relevant increases in MBF with vasodilation,[21] making it a potential diagnostic tool for the detection of ischemic heart disease.

Myocardial ischemia occurs when there is an imbalance between myocardial oxygen supply and myocardial metabolic oxygen demand, and is usually caused by CAD. The measurement of coronary sinus oxygen saturation has been used to detect global myocardial deoxygenation,[22,23] but this method is invasive, time-consuming, and impractical for serial measurements over time. Deoxyhemoglobin is paramagnetic, and blood oxygen level-dependent (BOLD) MRI can detect elevated deoxyhemoglobin levels in myocardial territories located downstream from stenotic coronary arteries.[24–26] Because ischemia is the initiator for the ischemic cascade, BOLD imaging may prove sensitive for the detection of CAD. Thus, the noninvasive measurement of myocardial deoxygenation with BOLD MRI may be a useful complement to existing MRI perfusion techniques.

In this study we performed the cardiac ASL method in healthy volunteers at both rest and stress using adenosine vasodilation, and we report MBF and MPR on both a global and per-segment basis. We also used a reference T_2-prep SSFP BOLD method to concurrently assess myocardial oxygenation in the same subjects.

MATERIALS AND METHODS

Experimental Methods

The study included 10 volunteers with no past medical history and no history of tobacco use. All volunteers were instructed to avoid caffeinated food and drinks for a period of 24 hours prior to the scan. Upon arrival to the MRI suite, one IV was placed (20G) in the antecubital vein for adenosine infusion. Adenosine was the only medication administered during the protocol. The study protocol was Institutional Review Board-approved, and written informed consent was obtained from all subjects.

All scans were performed on a 3T system (Signa Excite HDxt, GE Healthcare, Milwaukee, WI) using an 8-channel cardiac array. A localization scan was performed first, followed by steady state free precession (SSFP) long-axis and short-axis scans of the left ventricle to verify normal cardiac anatomy and function. A short axis slice at the mid-ventricular level was identified,[27] and a baseline image without the flow-sensitive inversion recovery (FAIR) labeling pulse was acquired to ensure the slice was properly prescribed without banding artifacts over the myocardium. If banding artifacts were present on the myocardium, a frequency scout scan was performed. The offset frequency that resulted in no banding artifact in the region of interest (myocardium) was recorded and used for subsequent scans. Breath-holds and cardiac triggering were used to minimize respiratory and cardiac motion, respectively. Single-gated myocardial ASL perfusion imaging was performed using FAIR with balanced steady state free precession (bSSFP) image acquisition.[19,28]

The ASL scan consisted of seven breath-holds. The first 5-second breath-hold was comprised of a baseline image (without labeling pulse) and an inversion check (pulsed label applied immediately before image acquisition). The next six 12-second breath-holds were each comprised of one control and one labeled image. The FAIR labeling inversion pulse was timed to occur at mid-diastole through plethysmograph gating (PG). Mid-diastole was estimated to be at 75% of the RR interval duration[29] and the PG trigger delay was set to this value minus 200 msec to account for circulation time from the R-wave to the fingertip.[30] The center of the acquisition window was set to occur one heartbeat (TI = 1RR) after the FAIR labeling pulse. Control and labeled images were acquired in the same breath-hold. Sequence parameters for single-gated myocardial ASL include echo time (TE) = 1.4 (1.3–1.5) msec, repetition time (TR) = 3.2 (3.0–3.5) msec, flip angle 50°, slice thickness = 10 mm, field of view 210 (160–260) mm, matrix size = 96 × 96 with parallel imaging GRAPPA rate 1.6, and 19-TR ramp-up and ramp-down pulses weighted by Kaiser–Bessel window were used to optimally minimize transient artifact and preserve longitudinal magnetization after image acquisition, respectively.[31] A fat-saturation pulse was applied immediately before the ramp-up pulses. A nonselective hyperbolic secant adiabatic inversion pulse was used for labeling. A 30 mm slice-selective inversion slab was used for the control image.

The BOLD scan was performed using a 50 msec adiabatic T_2-prep[24] and bSSFP image acquisition with the same sequence parameters as the ASL scan, using the same mid-ventricular level short axis slice. The BOLD scan consisted of two breathholds of ~13 seconds each. In each breath-hold, three T_2-prep bSSFP images were acquired with a 5-second time gap between images, resulting in a total of six averages for each BOLD scan.

After rest images were acquired, adenosine infusion was initiated at 140 mcg/kg/min for a total duration of 6 minutes. Stress imaging was started exactly 2 minutes after adenosine infusion was initiated, with ASL and BOLD scans performed sequentially in randomized order. A cardiologist was present to supervise all studies. Of 10 healthy subjects, one subject requested premature study termination due to claustrophobia before rest images were acquired, and one subject was unable to perform breath-holds during adenosine infusion, leaving eight complete rest and stress datasets for study analysis. Total scan time for completion of all stress ASL and BOLD scans was less than 3 minutes in all subjects.

Data Analysis

MBF was calculated in the same way as previously described.[28] All data processing was performed in MatLab (MathWorks, Natick, MA). After image reconstruction, the myocardium was manually segmented and resampled into polar coordinates using a spatiotemporal averaging filter.[32] MBF quantification was derived from Buxton's general kinetic model[33]:

$$MBF = \frac{C - L}{2 \cdot B \cdot TI \cdot \exp(-TI/T1)},$$

where C, L, and B refer to the mean myocardial signal in the control, labeled, and baseline images, TI represents the postlabeling

TABLE 1. Study Subject Baseline Characteristics

Subject	1	2	3	4	5	6	7	8	Mean ± SD
Age/sex	26 F	27 F	34 M	33 M	30 F	32 M	23 M	26 M	(Age) 28 ± 4
Systolic BP	110	121	118	114	107	132	129	126	120 ± 9
Diastolic BP	50	75	65	53	62	82	81	74	68 ± 12
Heart rate	46	73	81	74	84	78	66	71	72 ± 12

M = male; F = female; SD = standard deviation; BP = blood pressure.

delay time and was equal to the R-R interval, and T_1 is the longitudinal relaxation time of blood, which was assumed to be 1650 msec.[34] MPR was defined as the ratio of MBF_{stress} to MBF_{rest}.

The size of the spatial filter and the number of resampled segments could be freely chosen. Global MBF quantification was performed with a filter size of 2π and a single segment while a filter size of $\pi/3$ was used for per-segment analysis. Per-segment analysis was also performed for each subject. Each midventricular short-axis image was divided into six equiangular segments (inferoseptal, anteroseptal, anterior, anterolateral, inferolateral, and inferior) according to the middle-slice six segments of the American Heart Association 17-segment model.[27] Physiologic noise (PN) is a measure of the variability of measured MBF, and is measured in ml/g/min. PN is defined as the standard deviation (SD) of six repeated MBF measurements as described in Zun et al,[19] and represents all sources of variation in ASL measurements including methodological variability, short-term biological fluctuation, as well as cardiac and respiratory motion. Temporal SNR, defined as MBF/PN, was also calculated.

BOLD signal intensity (SI) index was calculated in the same way previously described[35] as the following equation:

$$\Delta SI(\%) = 100 \cdot \frac{SI_{strees} - SI_{rest}}{SI_{rest}},$$

where SI_{stress} and SI_{rest} are mean myocardial signal intensity at rest and stress, respectively. No segments were excluded from BOLD SI index analysis.

Statistical Analysis

Data normality was assessed using scatterplot and the Anderson–Darling test. Since the data were skewed, nonparametric data analyses were used. For global MBF change, the Wilcoxon signed rank test was used to assess the increase in MBF with adenosine. For segmental analysis, the data were first transformed into Wilcoxon ranking score, then the random effect model was used to assess intra- (increase within segment) and intersegment (either rest or stress between segments) variations for both MBF and PN. A significant interaction between segment and phase will indicate a change from rest to stress varied across segments; otherwise, a nonsignificant interaction will indicate the change from rest to stress being consistent across segments. Post-hoc comparisons across segments were conducted using the Kruskal–Wallis test, and between rest and stress for individual segments using Wilcoxon signed rank tests. Since eight post-hoc tests were conducted, an alpha level of 0.006 was used based on Bonferroni correction. Spearman correlation was used to compare BOLD SI % change to MPR, on both a per-segment and global basis. SAS 9.4 (Cary, NC) was used for all data analysis.

RESULTS

Study subjects consisted of five males and three females, age 23–34 years (Table 1). Figure 1 shows global MBF measurements at rest (blue) and stress (red) for each subject. Each bar represents the average MBF across the whole myocardium in the mid-ventricular slice. Error bars represent PN, which is one SD of measured MBF. The mean and SD of PN across all subjects was 0.19 ± 0.15 ml/g/min at rest and 0.52 ± 0.27 ml/g/min at stress. Global PN was 11 ± 7% and 12 ± 6% relative to the mean MBF at rest and stress, respectively. The average heart rate increased by 66% from 64 beats/min at rest to 97 beats/min during adenosine infusion.

The mean and SD of global MBF across all subjects was 1.64 ± 0.60 ml/g/min at rest and 4.45 ± 1.81 ml/g/min at stress, yielding an average MPR (MBF_{stress}/MBF_{rest}) of 2.72 ± 0.47. Figure 2 shows MPR for each subject. On the basis of a Wilcoxon Signed Rank test, the MBF increase with adenosine was statistically significant ($P < 0.001$). The measured global MBF range was 1.10–2.89 ml/g/min at rest and 2.75–8.26 ml/g/min at stress.

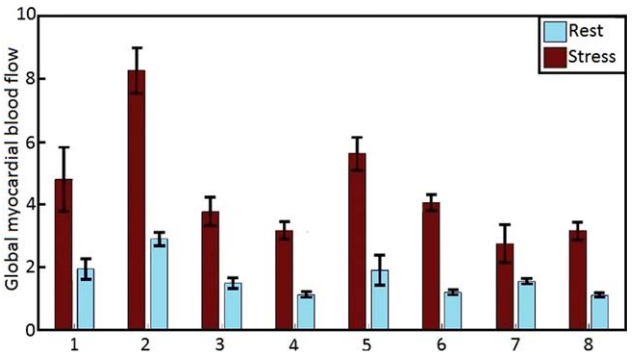

FIGURE 1: Global MBF at stress and rest for all eight subjects (horizontal axis). The mean and SD of global MBF across all subjects was 4.45 ± 1.81 ml/g/min at stress and 1.64 ± 0.60 ml/g/min at rest ($P < 0.0005$). Error bars represent ± 1 SD of measured PN.

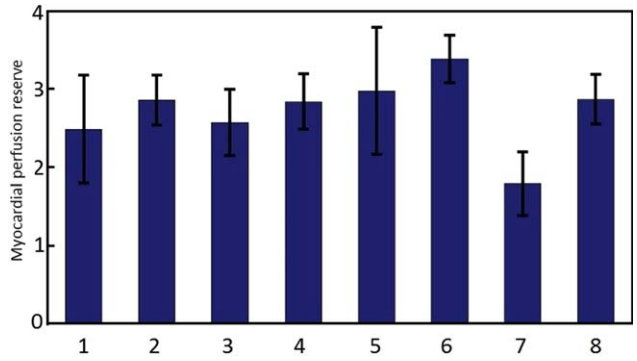

FIGURE 2: The mean and SD of global MPR across all eight subjects (horizontal axis) was 2.72 ± 0.47. Error bars represent error propagation of PN for MBF at rest and stress.

Per-segment analysis was performed for each segment (Fig. 3). Of 96 total left ventricle (LV) wall segments, five were excluded from per-segment analysis due to temporal signal-to-noise (tSNR) ratio <2. All five of these excluded segments were from rest ASL images; no stress ASL segments were excluded on the basis of tSNR. Three of the excluded segments were from one volunteer; the other two excluded segments were from different individuals. All five excluded segments were from different segment locations, with only the anterolateral wall having a per-segment rest and stress tSNR >2 in all subjects. Mean tSNR was similar at rest and stress with no significant per-segment differences (data not shown). The mean and SD for per-segment MBF was 1.75 ± 0.86 ml/g/min at rest and 4.58 ± 2.14 ml/g/min at stress ($P < 0.0001$), yielding a mean MPR of 3.02 ± 1.51 for all wall segments. The mean and SD for per-segment PN was 0.28 ± 0.20 ml/g/min at rest and 0.82 ± 0.58 ml/g/min at stress ($P < 0.0001$).

Figure 4 shows boxplots for MBF per specific LV wall segment (anteroseptal, anterior, anterolateral, inferolateral, inferior, and inferoseptal) at both rest and stress. On the basis of a Wilcoxon signed rank test, the MBF increase with adenosine was statistically significant ($P < 0.001$) for every LV wall segment. MPR for each wall segment (as well as rest and stress MBF) are summarized in Table 2.

There was no significant interaction found from mixed model for MBF ($P = 0.75$) and PN ($P = 0.12$). The post-hoc one-way Kruskal–Wallis tests were not statistically significant across segments for either rest ($P = 0.99$) or stress ($P = 0.67$) MBF, and rest ($P = 0.48$) or stress ($P = 0.3$) PN. The nonstatistically significant interaction test indicated the magnitudes of change from rest to stress were consistent across segments. Further pairwise tests for the difference from rest to stress were shown to be consistently significant for all segments using the Bonferroni corrected alpha level of 0.006.

The mean and SD of global BOLD SI change across all subjects was 14.23 ± 8.26%. The mean increase in per-segment BOLD SI index was 16.93 ± 7.88%. Spearman correlation was performed to compare BOLD SI change to MPR on both a segmental and global basis. No significant correlations were found (P = NS for all comparisons).

DISCUSSION

This study demonstrates the feasibility of measuring MBF and MPR on a per-segment basis by single-gated cardiac ASL. Second, this study demonstrates the feasibility of performing the ASL sequence and T_2-prepared SSFP BOLD imaging during a single adenosine infusion. There was a statistically significant increase in global MBF measurements with adenosine infusion (4.45 ± 1.80 ml/g/min) compared with rest (1.69 ± 0.59 ml/g/min), as expected for healthy volunteers, with a measured MPR of 2.75 ± 0.45. Of note, the mean stress and rest ASL MBF measurements in our study are higher than previously published results for global stress (3.67 ± 1.36 ml/g/min) and rest (0.97 ± 0.64 ml/g/min) ASL MBF,[22] which likely reflect patient population differences since the "normal" volunteers in the previous study had a mean age of 64 ± 12 years with an average of

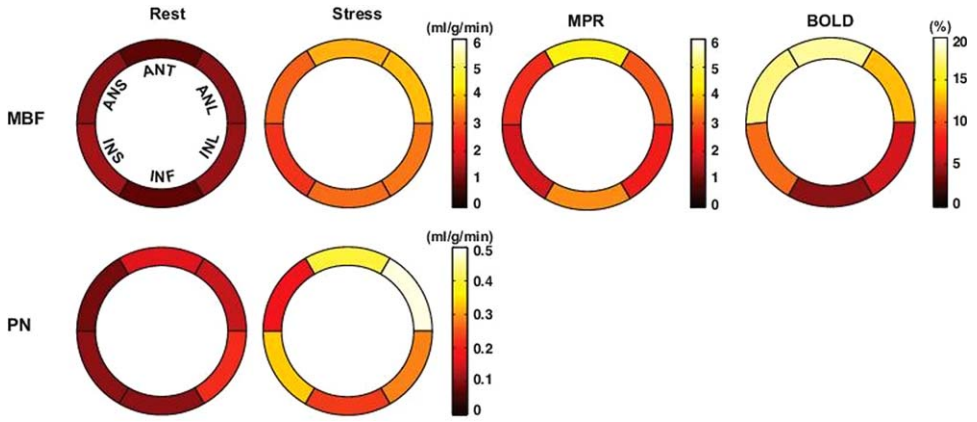

FIGURE 3: Side-by-side graphical comparison of segmental MBF at rest and stress, segmental PN at rest and stress, segmental MPR, and segmental BOLD SI % change in a single volunteer. ANS = anteroseptal, ANT = anterior, ANL = anterolateral, INS = inferoseptal, INF = inferior, INL = inferolateral.

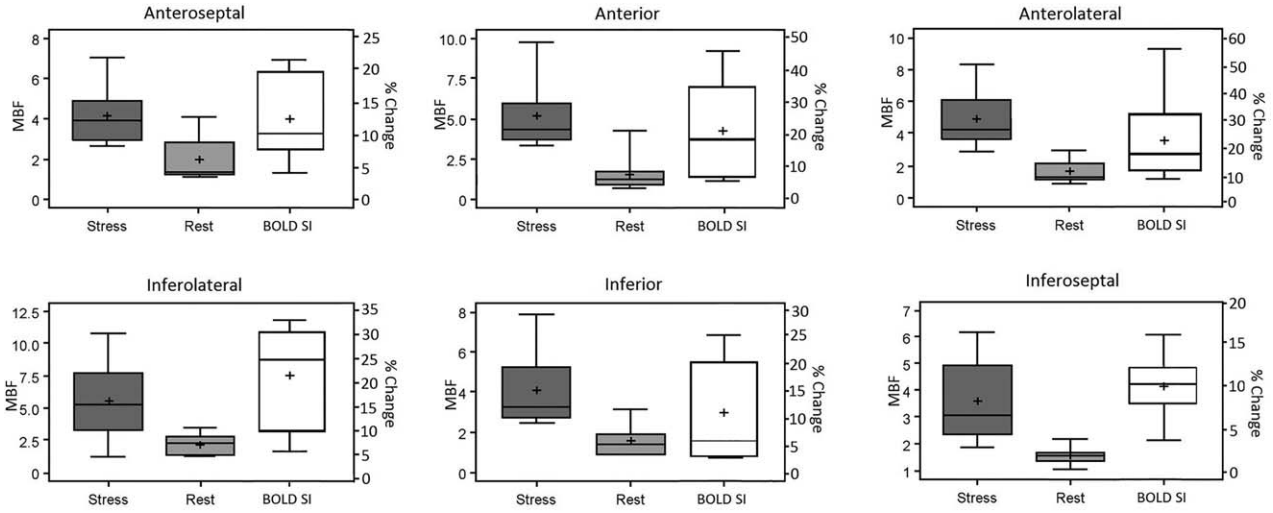

FIGURE 4: Boxplots for rest MBF, stress MBF, and BOLD SI % change per specific LV wall segment (anteroseptal, anterior, anterolateral, inferolateral, inferior, and inferoseptal) (horizontal line = mean; + = median; box = 25th and 75th percentile; error bars = maximum and minimum data points). On the basis of a Wilcoxon signed rank test, the MBF increase with adenosine was statistically significant ($P < 0.001$) for all LV wall segments. Left Y-axis = myocardial blood flow in ml/g/min. Right Y-axis = BOLD SI % change.

3.4 cardiovascular risk factors. Our findings also correlate with oxygen-15 positron emission tomography (PET) literature MBF values in normal individuals of 1.24 ± 0.19 ml/g/min at rest,[36] and 3.37 ± 1.25 to 5.05 ± 0.90 ml/g/min at stress.[37] Our derived measurements of global MPR in normal volunteers are consistent with previously published values in both the PET[38–41] and ASL literature.[22]

Furthermore, we extended on these earlier findings by reporting MBF and MPR on a per-segment basis, which is a necessary step to assess the clinical utility of cardiac ASL. Our results show differences in mean resting and stress perfusion among the various segments. For instance, one might anticipate that all healthy myocardial segments would have the same perfusion, whereas our study shows a stress anterior perfusion of 5.15 ml/g/min versus a stress inferoseptal perfusion of 3.6 ml/g/min. However, these segmental perfusion heterogeneities are also observed in the PET literature,[42] and may be explained by physiological factors such as differences in arterial transit time between the coronary branches, as well as cardiac and respiratory motion. Other nonphysiological factors, such as partial volume effects (contamination from ventricular blood pools) and off-resonance B_1-transmit inhomogeneity, may also be involved, although these effects are likely minimal. This study was not designed to investigate the diagnostic performance of cardiac ASL, but the per-segment results for MBF and MPR in our normal volunteers are consistent with normal values in the reported PET literature.[37,42,43] Additionally, our derived

TABLE 2. Per-segment MBF, MPR, and BOLD SI Change

LV wall segment	Rest MBF (ml/g/min)	Rest PN	Stress MBF (ml/g/min)	Stress PN	MPR	BOLD SI change (%)
Global	1.64 ± 0.60	0.19 ± 0.15	4.45 ± 1.81	0.52 ± 0.27	2.72 ± 0.47	14.23 ± 8.26
Anteroseptal	1.95 ± 1.11	0.29 ± 0.19	4.13 ± 1.46	0.75 ± 0.53	2.48 ± 0.51	12.97 ± 6.40
Anterior	1.55 ± 1.24	0.32 ± 0.25	5.15 ± 2.13	0.69 ± 0.33	4.44 ± 1.86	19.09 ± 14.88
Anterolateral	1.66 ± 0.74	0.31 ± 0.24	4.92 ± 1.91	0.85 ± 0.43	3.64 ± 1.90	23.06 ± 15.93
Inferolateral	2.18 ± 0.84	0.34 ± 0.19	5.58 ± 3.24	1.12 ± 0.64	4.06 ± 3.62	16.72 ± 13.12
Inferior	1.61 ± 0.76	0.20 ± 0.18	4.09 ± 1.98	0.63 ± 0.41	2.64 ± 0.84	10.09 ± 9.93
Inferoseptal	1.55 ± 0.34	0.19 ± 0.10	3.60 ± 1.65	0.94 ± 0.95	2.96 ± 2.25	8.86 ± 4.01

Values are reported as mean ± SD across subjects.
All MBF changes from rest to stress are statistically significant based on an alpha level of 0.006 after Bonferroni correction.
MBF = myocardial blood flow; MPR = myocardial perfusion reserve; BOLD SI = blood oxygen level-dependent signal intensity; LV = left ventricular; SD = standard deviation.

measurement for per-segment BOLD SI change was $16.93 \pm 7.88\%$, which is similar to previously reported values of $12.0 \pm 11.3\%$ (44) and 17.02% (35) in normal human subjects.

BOLD SI change did not significantly correlate with MPR in this study on either a global or segmental basis, even though the positive magnitude of MPR and BOLD SI % change seen globally and across myocardial segments in our study population are consistent with normal endothelial function and myocardial oxygenation in all test subjects. Likely reasons for this include the small sample size as well as the absence of a comparative disease-state arm. Further research will be required to validate the combined ASL-BOLD MRI methodology in a larger, mixed population including both normal and CAD patients.

Myocardial ischemia exists when there is an imbalance between myocardial oxygen supply and myocardial metabolic oxygen demand, and is usually caused by CAD. However, the correlation between myocardial ischemia and epicardial CAD, while strong, can also be nuanced. MPR is a measure of coronary endothelial vasoreactivity, while the causes of BOLD SI change are multifactorial and reflect blood flow, blood volume, and hemoglobin deoxygenation on a microvascular level. Uncoupling between MPR and BOLD SI change can occur in a variety of clinically relevant conditions. Normal stress perfusion can be accompanied by reduced stress oxygenation, as in patients with severe hypertension or left ventricular hypertrophy.[45,46] Conversely, impaired stress perfusion can occur with normal oxygenation when myocardial oxygen demand is downregulated, as in myocardial hibernation.[47]

Studies comparing BOLD MRI to either MRI or PET perfusion have shown that there are occasionally mismatches between deoxygenated myocardial territories and hypoperfused myocardial wall segments.[35,44] Myocardial autoregulation, adenosine triphosphate (ATP) usage, and myocardial blood volume have been proposed as possible etiologies for these observed deoxygenation-perfusion discrepancies. It is conceivable that the addition of oxygenation assessment to rest–stress perfusion protocols will enhance in the identification of physiologically significant coronary artery stenoses as well as the aforementioned clinically relevant conditions. However, it would be clinically laborious to perform PET perfusion imaging followed by BOLD MRI in the practice setting, as this would subject patients to considerable time and financial commitments in addition to the inconvenience of undergoing two sequential vasodilator stress tests, unless there is widespread clinical adoption of combined PET-MRI systems in the future. Several studies have shown correlation between MRI-derived MBF using gadolinium first-pass perfusion with BOLD MRI.[44,48,49] However, given real concerns over gadolinium exposure, neural gadolinium retention, and nephrogenic systemic fibrosis,[4] there is a clear clinical need for a contrast-free MR alternative. ASL MRI is a noninvasive MR technique that is capable of detecting clinically relevant changes in both MBF and MPR[21] and is free from gadolinium and radiation exposure. Although this study only included normal volunteers, the incorporation of BOLD MRI with cardiac ASL in a single rest–stress study protocol is technically and clinically feasible and worthy of further investigation and validation.

The study has several limitations. Only a small number of healthy subjects were recruited. Systematic evaluations of cardiac ASL on a larger cohort including patients with CAD are warranted for future study. There was no ground truth for MBF in this study. First-pass MRI and PET perfusion imaging may be used for comparison but were not available in this healthy volunteer cohort, but will be required in the future to validate ASL-derived estimates of both MBF and MPR. Current implementations of myocardial ASL suffer from greater noise and lower spatial resolution than state-of-the-art first-pass MRI, but these are not fundamental limitations of the ASL approach and are currently under investigation.[17,28] Another limitation of the current study is that we only used a single midventricular short-axis slice for imaging. Further technical innovations of the ASL technique, including the use of saturation labeling instead of inversion for the labeling pulse, may allow for complete data acquisition within two breath-holds instead of seven breath-holds, potentially allowing for whole-heart multislice acquisition with preserved SNR without sacrificing scan time. These and other similar efforts are currently under investigation.

In conclusion, this study demonstrates the feasibility of measuring MBF and MPR on a segmental basis by single-gated cardiac ASL. Second, this study demonstrates the feasibility of performing the ASL sequence and T_2-prepared SSFP BOLD imaging during a single adenosine infusion. This is expected to be valuable for the clinical applicability of cardiac ASL stress testing under pharmacologic stress.

ACKNOWLEDGMENTS

Contract grant sponsor: L.K. Whittier Foundation; contract grant number: 0003457-00001

REFERENCES

1. Salerno M, Beller GA. Noninvasive assessment of myocardial perfusion. Circ Cardiovasc Imaging 2009;2:412–424.
2. Cullen JHS, Horsfield MA, Reek CR, Cherryman GR, Barnett DB, Samani NJ. A myocardial perfusion reserve index in humans using first-pass contrast-enhanced magnetic resonance imaging. J Am Coll Cardiol 1999;33:1386–1394.
3. Greenwood JP, Maredia N, Younger JF, et al. Cardiovascular magnetic resonance and single-photon emission computed tomography for diagnosis of coronary heart disease (CE-MARC): a prospective trial. Lancet 2012;379:453–460.

4. Kuo PH, Kanal E, Abu-Alfa AK, Cowper SE. Gadolinium-based MR contrast agents and nephrogenic systemic fibrosis. Radiology 2007; 242:647–649.
5. Detre JA, Wang J, Wang Z, Rao H. Arterial spin-labeled perfusion MRI in basic and clinical neuroscience. Curr Opin Neurol 2009;22: 348–355.
6. Calamante F, Thomas DL, Pell GS, Wiersma J, Turner R. Measuring cerebral blood flow using magnetic resonance imaging techniques. J Cereb Blood Flow Metab 1999;19:701–735.
7. Watts JM, Whitlow CT, Maldjian JA. Clinical applications of arterial spin labeling. NMR Biomed 2013;26:892–900.
8. Belle V, Kahler E, Waller C, et al. In vivo quantitative mapping of cardiac perfusion in rats using a noninvasive MR spin-labeling method. J Magn Reson Imaging 1998;8:1240–1245.
9. Waller C, Kahler E, Hiller K, et al. Myocardial perfusion and intracapillary blood volume in rats at rest and with coronary dilatation: MR imaging in vivo with use of a spin-labeling technique. Radiology 2000; 215:189–197.
10. Kober F, Iltis I, Izquierdo M, et al. High-resolution myocardial perfusion mapping in small animals in vivo by spin-labeling gradient-echo imaging. Magn Reson Med 2004;51:62–67.
11. Streif JU, Nahrendorf M, Hiller K, et al. In vivo assessment of absolute perfusion and intracapillary blood volume in the murine myocardium by spin labeling magnetic resonance imaging. Magn Reson Med 2005;53:584–592.
12. Vandsburger MH, Janiczek RL, Xu Y, et al. Improved arterial spin labeling after myocardial infarction in mice using cardiac and respiratory gated Look-Locker imaging with fuzzy C-means clustering. Magn Reson Med 2010;63:648–657.
13. Campbell-Washburn AE, Price AN, Wells JA, Thomas DL, Ordidge RJ, Lythgoe MF. Cardiac arterial spin labeling using segmented ECG-gated look-locker FAIR: variability and repeatability in preclinical studies. Magn Reson Med 2013;69:238–247.
14. Troalen T, Capron T, Cozzone PJ, Bernard M, Kober F. Cine-ASL: a steady-pulsed arterial spin labeling method for myocardial perfusion mapping in mice. Part I. Experimental study. Magn Reson Med 2013; 70:1389–1398.
15. Capron T, Troalen T, Cozzone PJ, Bernard M, Kober F. Cine-ASL: a steady-pulsed arterial spin labeling method for myocardial perfusion mapping in mice. Part II. Theoretical model and sensitivity optimization. Magn Reson Med 2013;70:1399–1408.
16. Gutjahr FT, Kampf T, Winter P, et al. Quantification of perfusion in murine myocardium: A retrospectively triggered T1-based ASL method using model-based reconstruction. Magn Reson Med 2015;74: 1705–1715.
17. Poncelet B, Koelling T, Schmidt C, et al. Measurement of human myocardial perfusion by double-gated flow alternating inversion recovery EPI. Magn Reson Med 1999;41:510–519.
18. Northrup BE, McCommis KS, Zhang H, et al. Resting myocardial perfusion quantification with CMR arterial spin labeling at 1.5 T and 3.0 T. J Cardiovasc Magn Reson 2008;10:53.
19. Zun Z, Wong EC, Nayak KS. Assessment of myocardial blood flow (MBF) in humans using arterial spin labeling (ASL): Feasibility and noise analysis. Magn Reson Med 2009;62:975–983.
20. Wang DJJ, Bi X, Avants BB, Meng T, Zuehlsdorff S, Detre JA. Estimation of perfusion and arterial transit time in myocardium using free-breathing myocardial arterial spin labeling with navigator-echo. Magn Reson Med 2010;64:1289–1295.
21. Zun Z, Varadarajan P, Pai RG, Wong EC, Nayak KS. Arterial spin labeled CMR detects clinically relevant increase in myocardial blood flow with vasodilation. JACC Cardiovasc Imaging 2011;4:1253–1261.
22. Chierchia S, Brunelli C, Simonetti I, Lazzari M, Maseri A. Sequence of events in angina at rest: primary reduction in coronary flow. Circulation 1980;61:759–768.
23. Chierchia S, Lazzari M, Freedman B, Brunelli C, Maseri A. Impairment of myocardial perfusion and function during painless myocardial ischemia. J Am Coll Cardiol 1983;1:924–930.
24. Friedrich MG, Niendorf T, Schulz-Menger J, Gross CM, Dietz R. Blood oxygen level-dependent magnetic resonance imaging in patients with stress-induced angina. Circulation 2003;108:2219–2223.
25. Wacker CM, Hartlep AW, Pfleger S, Schad LR, Ertl G, Bauer WR. Susceptibility-sensitive magnetic resonance imaging detects human myocardium supplied by a stenotic coronary artery without a contrast agent. J Am Coll Cardiol 2003;41:834–840.
26. Shea SM, Fieno DS, Schirf BE, et al. T2-prepared steady-state free precession blood oxygen level-dependent MR imaging of myocardial perfusion in a dog stenosis model. Radiology 2005;236: 503–509.
27. Cerqueira MD, Weissman NJ, Dilsizian V, et al. Standardized myocardial segmentation and nomenclature for tomographic imaging of the heart: a statement for healthcare professionals from the Cardiac Imaging Committee of the Council on Clinical Cardiology of the American Heart Association. Circulation 2002;105:539–542.
28. Do HP, Jao TR, Nayak KS. Myocardial arterial spin labeling perfusion imaging with improved sensitivity. J Cardiovasc Magn Reson 2014;16: 15.
29. Otton JM, Phan J, Feneley M, Yu C, Sammel N, McCrohon J. Defining the mid-diastolic imaging period for cardiac CT — lessons from tissue Doppler echocardiography. BMC Med Imaging 2013;13:5.
30. Allen J, Murray A. Age-related changes in peripheral pulse timing characteristics at the ears, fingers and toes. J Hum Hypertens 2002; 16:711–717.
31. Le Roux P. Simplified model and stabilization of SSFP sequences. J Magn Reson 2003;163:23–37.
32. Jao T, Zun Z, Varadarajan P, Pai RG, Nayak KS. Mapping of myocardial ASL perfusion and perfusion reserve data. In: Proc 19th Annual Meeting ISMRM, Montreal; 2011. p 1339.
33. Buxton RB, Frank LR, Wong EC, Siewert B, Warach S, Edelman RR. A general kinetic model for quantitative perfusion imaging with arterial spin labeling. Magn Reson Med 1998;40:383–396.
34. Lu H, Clingman C, Golay X, van Zijl P. Determining the longitudinal relaxation time (T1) of blood at 3.0 Tesla. Magn Reson Med 2004;52: 679–682.
35. Karamitsos TD, Leccisotti L, Arnold JR, et al. Relationship between regional myocardial oxygenation and perfusion in patients with coronary artery disease: insights from cardiovascular magnetic resonance and positron emission tomography. Circ Cardiovasc Imaging 2010;3: 32–40.
36. Wyss CA, Koepfli P, Mikolajczyk K, et al. Bicycle exercise stress in PET for assessment of coronary flow reserve: repeatability and comparison with adenosine stress. J Nucl Med 2003;44:146–154.
37. Klocke FJ, Lee DC. Absolute myocardial blood flow emerging role in coronary pathophysiology and clinical disease. JACC Cardiovasc Imaging 2011;4:999–1001.
38. Kaufmann PA, Gnecchi-Ruscone T, Schafers KP, Luscher TF, Camici PG. Low density lipoprotein cholesterol and coronary microvascular dysfunction in hypercholesterolemia. J Am Coll Cardiol 2000;36:103–109.
39. Kaufmann PA, Rimoldi OE, Gnecchi-Ruscone T, Luscher TF, Camici PG. Systemic nitric oxide synthase inhibition improves coronary flow reserve to adenosine in patients with significant stenoses. Am J Physiol Heart Circ Physiol 2007;293:H2178–2182.
40. Wu YW, Chen YH, Wang SS, et al. PET assessment of myocardial perfusion reserve inversely correlates with intravascular ultrasound findings in angiographically normal cardiac transplant recipients. J Nucl Med 2010;51:906–912.
41. Knesaurek K Machac J, Zhang Z. Repeatability of regional myocardial blood flow calculation in 82Rb PET imaging. BMC Med Phys 2009; 9:2.

42. Chareonthaitawee P, Kaufmann P, Rimoldi O, Camici P. Heterogeneity of resting and hyperemic myocardial blood flow in healthy humans. Cardiovasc Res 2001;50:151–161.

43. Packard RR, Huang SC, Dahlbom M, Czernin J, Maddahi J. Absolute quantitation of myocardial blood flow in human subjects with or without myocardial ischemia using dynamic flurpiridaz F 18 PET. J Nucl Med 2014;55:1438–1444.

44. Arnold JR, Karamitsos TD, Bhamra-Ariza P, et al. Myocardial oxygenation in coronary artery disease: insights from blood oxygen level-dependent magnetic resonance imaging at 3 Tesla. J Am Coll Cardiol 2012;59:1954–1964.

45. Beache GM, Herzka DA, Boxerman JL, et al. Attenuated myocardial vasodilator response in patients with hypertensive hypertrophy revealed by oxygenation-dependent magnetic resonance imaging. Circulation 2001;104:1214–1217.

46. Karamitsos TD, Dass S, Suttie J, et al. Blunted myocardial oxygenation response during vasodilator stress in patients with hypertrophic cardiomyopathy. J Am Coll Cardiol 2013;61:1169–1176.

47. Fallavollita JA, Malm BJ, Canty JM Jr. Hibernating myocardium retains metabolic and contractile reserve despite regional reductions in flow, function, and oxygen consumption at rest. Circ Res 2003;92:48–55.

48. Jahnke C, Gebker R, Manka R, et al. Navigator-gated 3D blood oxygen level-dependent CMR at 3.0-T for detection of stress-induced myocardial ischemic reactions. JACC Cardiovasc Imaging 2010;3:375–384.

49. Bernhardt P, Manzke R, Bornstedt A, et al. Blood oxygen level-dependent magnetic resonance imaging using T2-prepared steady-state free-precession imaging in comparison to contrast-enhanced myocardial perfusion imaging. Int J Cardiol 2011;147:416–419.